Journal of Alloys and Compounds 711 (2017) 229–234

Contents lists available at ScienceDirect

Journal of Alloys and Compounds

journal homepage: http://www.elsevier.com/locate/jalcom

Spin-polarized antiferromagnetic CaCoSO single crystal: First-principles study

A.H. Reshak [a, b, *]

[a] New Technologies – Research Centre, University of West Bohemia, Univerzitni 8, 306 14 Pilsen, Czech Republic
[b] School of Material Engineering, University Malaysia Perlis, 01007 Kangar, Perlis, Malaysia

ARTICLE INFO

Article history:
Received 7 March 2017
Received in revised form
31 March 2017
Accepted 1 April 2017
Available online 4 April 2017

Keywords:
Spin-polarization
Electronic materials
Magnetic moment

ABSTRACT

Comprehensive spin-polarized calculations were performed for the recently synthesized antiferromagnetic CaCoSO single crystal based on the full-potential method plus Hubbard Hamiltonian. The experimental lattice parameters of the CaCoSO single crystal were optimized and the experimental atomic positions were relaxed so as to minimize the forces acting on the atoms. The calculations show that the spin-up (-down) channels exhibit a direct energy band gap Γ_v- Γ_c (K_v-K_c) of about 2.187 (1.187) eV and the spin-polarized antiferromagnetic CaCoSO single crystal exhibits an indirect energy band gap (Γ_v- K_c) of about 0.4 eV. The obtained magnetic moment of 3d electrons within the Co sphere (2.56 μB) is the highest among the others and agrees well with the measured ones (2.75 μB). Further, the charge density distribution of the spin-polarized valence electrons for the spin-up and spin-down channels were investigated in two crystallographic planes. The calculated bond lengths and angles show good agreement with the measured ones.

1. Introduction

The oxide chalcogenides compounds have been of considerable interest for several applications, for instance, as p-type transparent conductors [1–6]. Among these oxide chalcogenides compounds is the CaCoSO compound, which has been recently synthesized from CaO, Co and S at 900 °C [7]. It has been reported that the CaCoSO is isostructural with CaZnSO, BaCoSO and CaFeSO [7–11]. It is noted that in the CaCoSO compound, the ordering of the O^{2-} and S^{2-} anions forms layered structures with segregation of metal cations [7]. The recently synthesized CaCoSO single crystal crystallizes in hexagonal symmetry with the $P6_3mc$ space group. The cell parameters of CaCoSO are a = b = 3.7415 (8) Å, c = 11.106 (2) Å, V = 134.64 (6) $Å^3$ and Z = 2, at room temperature [7]. Using the x-ray diffraction data of the recently synthesized antiferromagnetic CaCoSO single crystal obtained by Salter et al. [7], we have performed comprehensive density functional calculations based on the full-potential method within the generalized gradient approximation (PBE-GGA) plus Hubbard Hamiltonian (U) to support the experimental findings of Salter et al. [7]. The obtained theoretical results agree well with the measured ones.

2. Calculation methods and structural details

The present calculations were performed within density functional theory (DFT) employing the *ab-initio* LAPW + lo full-potential method utilizing the Wien2k code [12]. The full-potential method within the generalized gradient approximation (PBE-GGA) [13] were used to optimize the geometrical structure. It has been found that in CaCoSO single crystals, the electrons are highly localized; thus Coulomb repulsion between the electrons in open shells should be taken into account. It is well known that there is no exchange correlation functional that can include this in an orbital independent way; a simpler approach is to add the Hubbard-like on-site repulsion to the Kohn-Sham Hamiltonian. This is known as a DFT + U (U-Hubbard Hamiltonian) calculation. There are different ways in which this can be implemented; here we used the method of Anisimov et al. [14] and Liechtenstein et al. [15], where the Coulomb (U) and exchange (J) parameters were used. The tetrahedron method within Blochl corrections [16] was used to calculate the density of states. Using FPLAPW + lo [12,17,18] within GGA + U the electronic band structure was calculated. We applied the U on the 3d orbitals of the Co atom. Several U values were used to obtain a qualitative agreement with experimental

* New Technologies – Research Centre, University of West Bohemia, Univerzitni 8, 306 14 Pilsen, Czech Republic.
E-mail address: maalidph@yahoo.co.uk.

http://dx.doi.org/10.1016/j.jallcom.2017.04.002
0925-8388/

data. The U value used here was 0.20 Ry for Co-3d.

To insure that no charge leakage is left out of the atomic sphere cores, the minimum radius of the muffin-tin spheres (R_{MT}) values are set as 2.03 a.u. for Ca atoms, 1.78 a.u. for Co atoms, 1.87 a.u. for S atoms and 1.53 a.u. for O atoms. The R_{MT}'s were chosen in such a way that the spheres did not overlap. The basis functions inside the interstitial region were expanded up to $R_{MT} \times K_{max} = 7.0$ and inside the atomic spheres for the wave function, in order to achieve the total energy convergence. The potential for the construction of basis functions inside the sphere of the muffin tin was spherically symmetric, whereas outside the sphere it was constant [19]. The maximum value of $\boldsymbol{l}$ is taken as $\boldsymbol{l}_{max} = 10$, while the charge density is Fourier expanded up to $G_{max} = 12.0(a.u)^{-1}$. In current calculations the self-consistency was obtained using 900 k points in the irreducible Brillouin zone (IBZ). The self-consistent calculations were converged since the total energy of the system was stable within 0.00001 Ry. The spin-polarized electronic band structure, density of states, spin magnetic moments, and valence electrons charge density distribution were calculated using 20000 k points in the IBZ, as accurate calculations require a dense sampling of the BZ. The DFT method has been proven to be one of the most accurate method for the computation of the electronic structure of solids [20,21].

3. Results and discussion

The obtained lattice constant and the atomic positions in comparison with the experimental data [7] are listed in Table 1. Following Table 1, one can see that the relaxed geometrical structure shows good agreement with the reported x-ray diffraction data [7]. The relaxed structure used in this manuscript can be find as crystallographic cif file in the Supplemental material. The optimized crystal structure of the CaCoSO single crystal is shown in Fig. 1, which show that the crystal structure of CaCoSO has polar layers in the *ab* plane of S atom-vertex sharing CoS_3O tetrahedral that are separated by Ca ions of the CaS_4O_3 octahedral.

To verify the contribution of each atom in the antiferromagnetic CaCoSO single crystal, the projected density of states associated with the total density of states are investigated and shown in Fig. 2a-d. The projected density of states reveals that in the spin-down channel the Co-4s/3p/3d, S-3p, O-2s/2p and Ca-3p orbitals form the structure in the energy confined between 0.4 eV and 3.0 eV, resulting in a band gap reduction by around 1.0 eV. Whereas in the spin-up channel this structure vanishes, resulting in opening a bigger energy band gap. The calculated energy band gap for the spin-up channel is about 2.187 eV, while the spin-down one is about 1.187 eV. Thus, the spin-polarized antiferromagnetic CaCoSO single crystal exhibits an energy band gap of about 0.4 eV. To date, no experimental or theoretical data for the energy band gap are

Table 1
Optimized lattice constants and the atomic positions of CaCoSO single crystal in comparison with the experimental data [7].

Cell parameters (Å)		a		b		c
Exp.		3.7524 (9)[a]		3.7524 (9)[a]		11.138 (3)[a]
This work		3.7520		3.7520		11.136
Atomic positions						
Atom	x exp.[a]	x optim.	y exp.[a]	y optim.	z exp.[a]	z optim.
Ca	1/3	1/3	2/3	2/3	0.2682 (3)	0.2747
Co	0.0	0.0	0.0	0.0	0.0	0.0
S	2/3	2/3	1/3	1/3	0.0789 (4)	0.0614
O	0.0	0.0	0.0	0.0	0.3326 (3)	0.3357

[a] Ref. Exp. [7] (Experimental result).

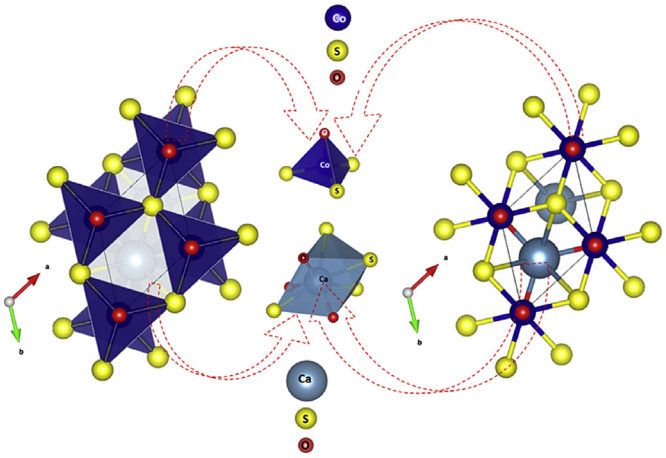

Fig. 1. The crystal structure of antiferromagnetic CaCoSO single crystal which show the CaS_4O_3 octahedral and the CoS_3O tetrahedral. The crystal structure of CaCoSO has polar layers in the *ab* plane of S atom-vertex sharing CoS_3O tetrahedral that are separated by Ca ions of the CaS_4O_3 octahedral.

available in the literature to be compared with our theoretical results. To obtain further insight into the type of states associated with each orbital, the orbital-decomposed partial density of states of the Co-3d state in CaCoSO is shown in Fig. 2d, which shows the degenerate Co-3dxz/3dyz, Co-3dxy/3dx^2-y^2 and Co-3dz^2. It has been reported that the distortion in CaCoSO from CoS_3O tetrahedral is relatively small and the Co^{2+} coordination environment has C_{3v} symmetry [7] thus, the occupancy of the Co-3d levels will be as; Co-3dz^2 which is comparable in energy to the higher-lying degenerate Co-3dxz/3dyz pair and the degenerate Co-3dxy/3dx^2−y^2 pair will lie low in energy. Furthermore, the calculated projected density of states reveals the hybridization between the orbitals, for instance, the Co-3d orbital strongly hybridized with the S-3p and O-2p orbitals, and the Co-4s orbital hybridized with Ca-4s/3p, Co-3p and O-2s orbitals. The hybridization may lead to the formation of covalent bonding; the strength of the covalency relating to the strength of the hybridization [22].

In order to verify the results of the projected density of states, the spin-polarized electronic band structure for the spin-up/down channels are calculated and presented in Fig. 3(a–d) along with the first BZ. It is clear that the spin-up/down channels of the CaCoSO single crystal possesses a direct energy band gap as the top of the valence band (TVB) and the bottom of the conduction band (BCB) for the spin-up channel are situated at the center (0.0, 0.0, 0.0) of the BZ, whereas for the spin-down channel the TVB and BCB are located at K (1/3, 1/3, 0.0) symmetry points of the BZ. The calculated spin-polarized electronic band structure of the antiferromagnetic CaCoSO single crystal shows that the TVB is located at Γ, whereas the BCB is situated at K, resulting in an indirect energy band gap of about 0.4 eV (Fig. 3d). Further, the spin-down electronic band structure reveals the appearance of the Co-4s/3p/3d, S-3p, O-2s/2p and Ca-3p bands in the energy region just above the Fermi level (E_F), which confirms the occurrence of a band gap reduction in the spin-down channel. Also, it shows that the Co-3d, O-2p and S-3p bands were split by around 0.5 eV from the valence bands. Therefore, the spin-polarization causes a band gap reduction in the spin-down channel and shifts the TVB and BCB to be located at (1/3, 1/3, 0.0) symmetry points. We set the zero-point of energy at Fermi level (E_F).

We obtained the values of the spin magnetic moments for the atom resolved within the muffin-tin spheres and in the interstitial sites. These values in the unit of μB are listed in Table 2. The

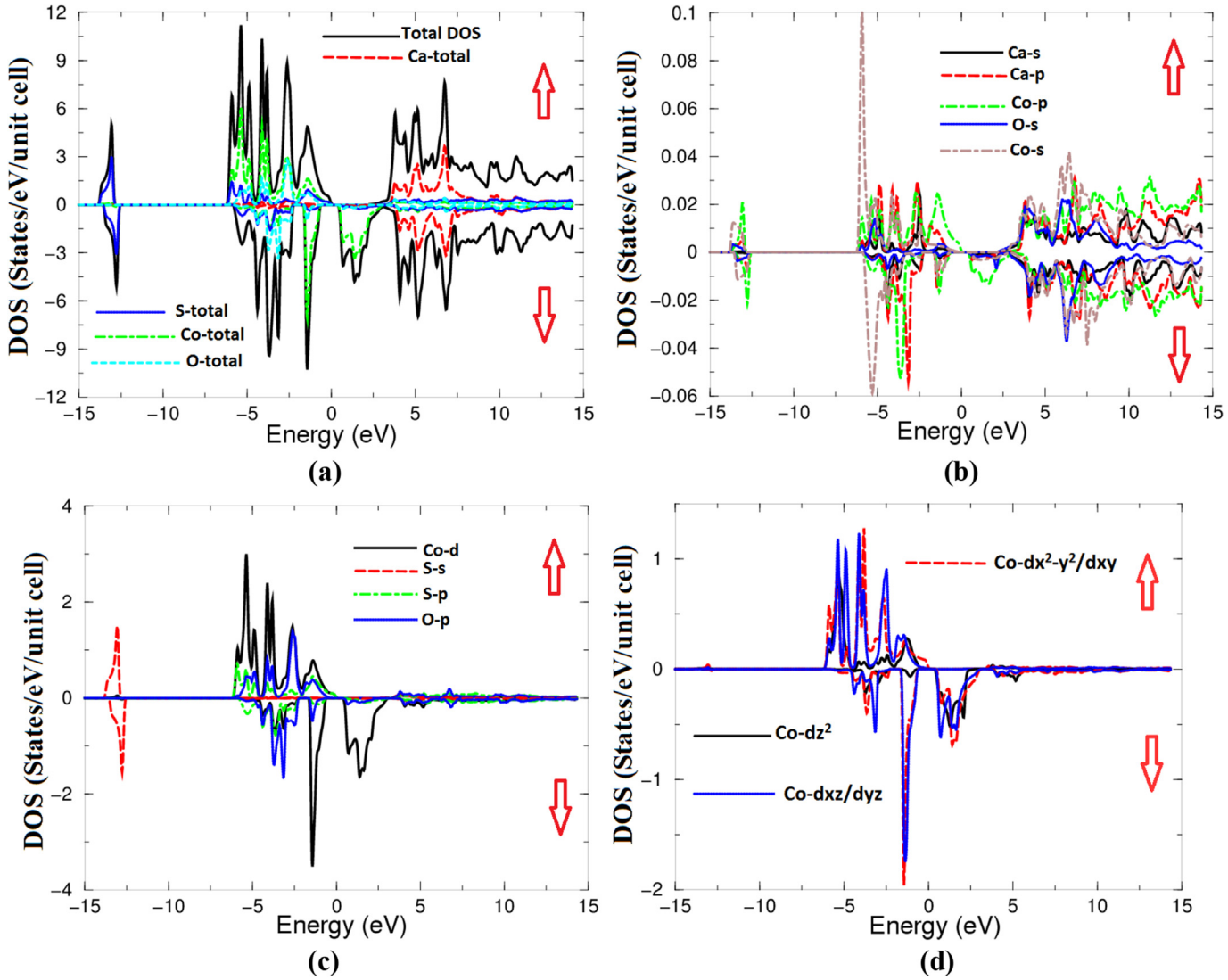

Fig. 2. Spin-polarized projected density of states associated with the total density of states of antiferromagnetic CaCoSO single crystal; (a) total density of states for CaCoSO along with the total density of states for Ca, Co, S and O atoms for spin-up and spin down channels; (b) Ca-s/p, Co-s/p and O-s partial density of states for spin-up and spin down channels; (c) Co-d, S-s/p and O-p partial density of states for spin-up and spin down channels; (d) Co-dx^2-y^2/dxy, Co-dz^2 and Co-dxz/dyz partial density of states for spin-up and spin down channels. The arrow ↑ denotes the spin-up and ↓ denotes the spin-down.

obtained spin magnetic moments are in accordance with the Slater-Pauling rule. Table 2 shows that the magnetic moment of 3d electrons within the Co sphere (2.56 μB) is the highest among the others. The calculated magnetic moment agrees well with the measured ones (2.75 μB) [7]. It has been reported that in CaCoSO there are three unpaired electrons and no first order orbital contribution to the moment [7]. Due to the considerable covalency, the ordered moment will be lower than that of the spin-only (3.0 μB) [7]. We should emphasize that the calculated magnetic moment is smaller than the experimental value by around 0.19 μB, which is attributed to the DFT limitations.

The spin-polarized valence electrons charge density distribution for the spin-up and spin-down channels were investigated in (1 0 0) and (1 0 1) crystallographic planes. The (1 0 0) plane (Fig. 4a and b) exhibits O and Ca atoms, the O atoms are surrounded by blue uniform spheres, whereas the (1 0 1) plane (Fig. 4c and d) shows all atoms and the charge distribution around O, S and Co atoms. According to Pauling scale, the electro-negativity of O, S, Co and Ca are 3.44 > 2.58 > 1.88 > 1.00, which show that the O atom possesses the highest electro-negativity among the others. For the description of the character of the bonding the difference of the electro-negativity (X_A-X_B) is crucial [23], where X_A and X_B denotes the electro-negativity of the A and B atoms in general. With increasing the difference the ionic character (P) of the bonding increases. The percentage of the ionic character (P) of the bonding can be obtained follow the relation [23]:

$$P(\%) = 16(X_A\text{-}X_B)+3.5(X_A\text{-}X_B)^2. \quad (1)$$

The calculated values of the ionic character are given in Table 3. It is clear that the Co atom in CoS_3O tetrahedral forms mostly covalent and partially ionic bonding with S and O atoms, and the calculated Co—O bond length (1.857 Å) is shorter than that of the Co—S (2.331 Å) see Fig. 4e, f and Table 3. Whereas in the CaS_4O_3 octahedral, the Ca atom forms mostly ionic and partially covalent bonds with O, and mostly covalent and partially ionic with S atoms (see Fig. 4 g and Table 3). The calculated Ca—O bond length (2.274 Å) is shorter than that of the Ca—S (3.012 Å). The crystallographic

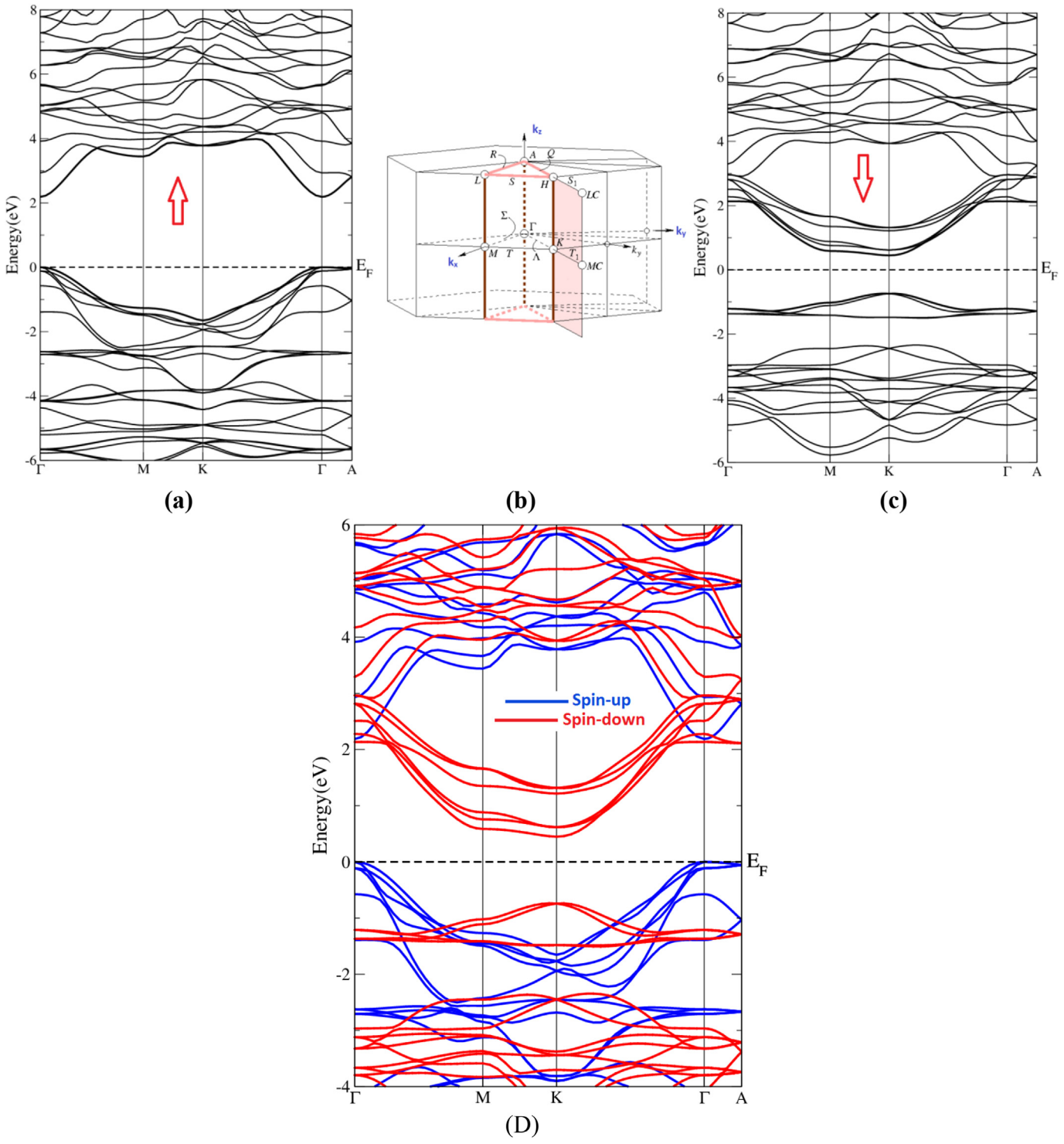

Fig. 3. Spin-polarized electronic band structure of antiferromagnetic CaCoSO single crystal; (a) Spin-up; (b) First BZ; (c) Spin-down; (d) Spin-polarized electronic band structure. The arrow ↑ denotes the spin-up and ↓ denotes the spin-down. We set the zero-point of energy at Fermi level.

Table 2
Calculated atom-resolved spin magnetic moment (in μB) along with the experimental result [7].

Ca (μB)	Co (μB)	S (μB)	O (μB)	Interst. (μB)
0.00869	2.56121 2.75[a]	0.12608	0.13735	0.73283

[a] Ref. [7] (Experimental result).

planes show that a charge transfer towards O and S atoms occurs, as it is shown by the blue uniform spheres surrounding the O and S atoms indicating the maximum charge accumulated according to the thermo-scale (Fig. 4h). To provide a quantities comparison between theoretical and experimental values of the bond lengths and angles, we have calculated the bond lengths and angles for the CaCoSO single crystal as shown in Table 4. It is clear that there is

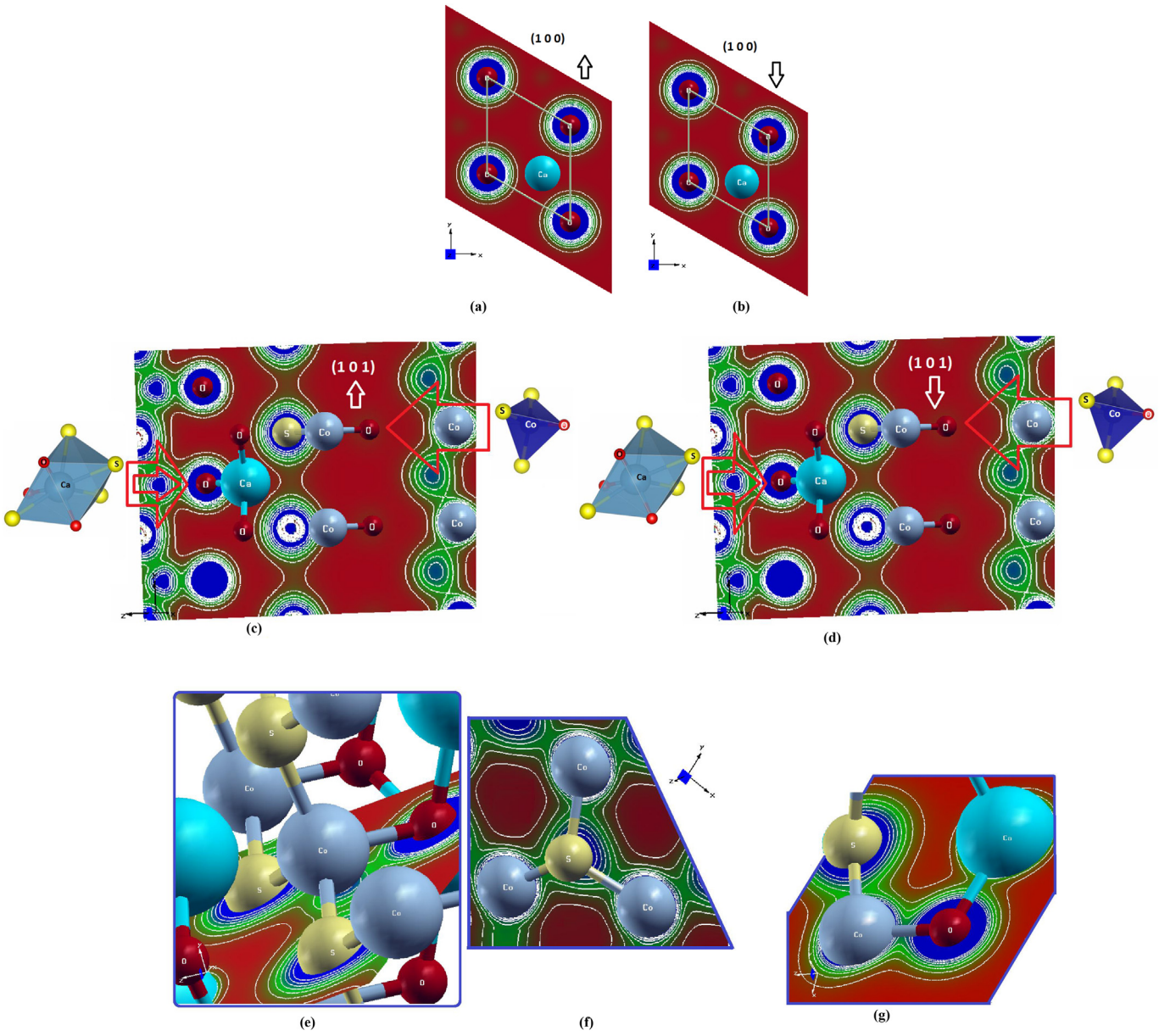

Fig. 4. Spin-polarized valence electrons charge density distribution in two crystallographic planes (1 0 0) and (1 0 1) for the antiferromagnetic CaCoSO single crystal; (a) (1 0 0) crystallographic plane for spin-up; (b) (1 0 0) crystallographic plane for spin-down; (c) (1 0 1) crystallographic plane for spin-up; (d) (1 0 1) crystallographic plane for spin-down; (e,f) show the CoS_3O tetrahedral and the charge distribution around S, O and Co atoms; (g) show the charge distribution around Ca, Co, S and O; (h) thermo-scale. The arrow ↑ denotes the spin-up and ↓ denotes the spin-down.

Table 3
The calculated values of the ionic character.

Bonds	P (%)
Co–O	33.47
Co–S	12.91
Ca–O	59.87
Ca–S	34.01

good agreement with the experimental data [7] and confirms that the Co–O (Ca–O) bond length is shorter than that of the Co–S (Ca–S). The three angles of O–Co–S in the CoS_3O tetrahedral are equal also the three S–Co–S angles are equal too (Fig. 1) which reveals the symmetry of the CoS_3O tetrahedral in good agreement with the experimental data [7]. The bond lengths and the two crystallographic planes reveal that the CaCoSO single crystal possesses considerable anisotropy.

4. Conclusions

The x-ray diffraction data of the recently synthesized antiferromagnetic CaCoSO single crystal were optimized using the full-potential method within PBE-GGA. The spin-polarized electronic band structure, the projected density of states, the spin magnetic moments and the valence electrons charge density distribution were calculated using PBE-GGA in combination with appropriate on-site Coulomb interactions to describe the electron exchange and correlation potentials. Calculations show that the spin-up (spin-down) channels exhibit a direct energy band gap of about 2.187 (1.187) eV and the spin-polarized antiferromagnetic CaCoSO single

Table 4
The calculated bond lengths and bond angles in comparison with experimental data [7].

	Exp.	Calc.
Bond lengths (Å)		
Ca–O	2.276 (2)	2.274
Ca–S	3.014 (4)	3.012
Co–O	1.859 (3)	1.857
Co–S	2.331 (2)	2.329
Bond Angles (°)		
O–Co–S	112.1 (1)	112.0
S–Co–S	106.8 (1)	106.6

crystal exhibits an indirect energy band gap of about 0.4 eV. The obtained values of the spin magnetic moments for the atom resolved within the muffin-tin spheres and in the interstitial sites show that the magnetic moment of Co-3d (2.56 μB) is the highest and agrees well with the measured ones (2.75 μB). It has been found that Co forms covalent bonding with S and O atoms and the Co–O bond length is shorter than that of the Co–S. The crystallographic planes show that a charge transfer towards O and S atoms occurs, as it is shown by the blue uniform spheres surrounding the O and S atoms indicating the maximum charge accumulated according to the thermo-scale. The calculated bond lengths and angles of the CaCoSO single crystal show good agreement with the experimental data.

Acknowledgments

The result was developed within the CENTEM project, reg. no. CZ.1.05/2.1.00/03.0088, co-funded by the ERDF as part of the Ministry of Education, Youth and Sports OP RDI program and, in the follow-up sustainability stage, supported through CENTEM PLUS (LO1402) by financial means from the Ministry of Education, Youth and Sports under the National Sustainability Program I. Computational resources were provided by MetaCentrum (LM2010005) and CERIT-SC (CZ.1.05/3.2.00/08.0144) infrastructures.

Appendix A. Supplementary data

Supplementary data related to this article can be found at http://dx.doi.org/10.1016/j.jallcom.2017.04.002.

References

[1] K. Ueda, S. Inoue, S. Hirose, H. Kawazoe, H. Hosono, Appl. Phys. Lett. 77 (2000) 2701–2703.
[2] Y. Kamihara, T. Watanabe, M. Hirano, H.J. Hosono, Am. Chem. Soc. 130 (2008) 3296–3297.
[3] S.J. Clarke, P. Adamson, S.J.C. Herkelrath, O.J. Rutt, D.R. Parker, M.J. Pitcher, C.F. Smura, Inorg. Chem. 47 (2008) 8473–8486.
[4] S.A. Petrova, V.P. Mar'evich, R.G. Zakharov, E.N. Selivanov, V.M. Chumarev, L. Yu Udoeva, Dokl. Chem. 393 (2003) 255–258.
[5] T. Sambrook, C.F. Smura, S.J. Clarke, K.M. Ok, P.S. Halasyamani, Inorg. Chem. 46 (2007) 2571–2574.
[6] S. Broadley, Z.A. Gal, F. Cora, C.F. Smura, S. Clarke, J. Inorg. Chem. 44 (2005) 9092–9096.
[7] J.T. Salter Edward, N. Blandy Jack, J. Clarke Simon, Inorg. Chem. 55 (2016) 1697–1701.
[8] E.N. Selivanov, V.M. Chumarev, R.I. Gulyaeva, V.P. Mar'evich, A.D. Vershinin, A.A. Pankratov, E.S. Korepanova, Inorg. Mater 40 (2004) 845–850.
[9] C. Delacotte, O. Perez, A. Pautrat, D. Berthebaud, S. Hebert, E. Suard, D. Pelloquin, A. Maignan, Inorg. Chem. 54 (2015) 6560–6565.
[10] S.F. Jin, Q. Huang, Z.P. Lin, Z.L. Li, X.Z. Wu, T.P. Ying, G. Wang, X.L. Chen, Phys. Rev. B Condens. Matter Mater. Phys. 91 (2015) 094420.
[11] M. Valldor, U.K. Rössler, Y. Prots, C.Y. Kuo, J.C. Chiang, Z.W. Hu, T.W. Pi, R. Kniep, L.H. Tjeng, Chem. - Eur. J. 21 (2015) 10821–10828.
[12] P. Blaha, K. Schwarz, G.K.H. Madsen, D. Kvasnicka, J. Luitz, WIEN2k, an Augmented Plane Wave Plus Local Orbitals Program for Calculating Crystal Properties, Vienna University of Technology, Austria, 2001.
[13] J.P. Perdew, S. Burke, M. Ernzerhof, Phys. Rev. Lett. 77 (1996) 3865.
[14] V.I. Anisimov, I.V. Solvyev, M.A. Korotin, M.T. Czyzyk, C.A. Sawatzky, Phys. Rev. B 48 (1993) 16929.
[15] A.I. Liechtenstein, V.I. Anisimov, J. Zaanen, Phys. Rev. B 52 (1995) R5467.
[16] P.E. Blochl, O. Jepsen, O.K. Andersen, Phys. Rev. B 49 (1994) 16223–16233.
[17] O.K. Andersen, Phys. Rev. B 12 (1975) 3060.
[18] J.P. Perdew, Y. Wang, Phys. Rev. B 45 (1992) 13244.
[19] K. Schwarz, P. Blaha, Solid state calculations using WIEN2k, Comput. Mater. Sci. 28 (2003) 259–273.
[20] H. Huang, Y. He, X. Li, M. Li, C. Zeng, F. Dong, X. Du, T. Zhangd, Y. Zhang, J. Mater. Chem. A 3 (2015) 24547–24556.
[21] H. Huang, Y. He, Z. Lin, L. Kang, Y. Zhang, J. Phys. Chem. C 117 (2013) 22986–22994.
[22] F. Wu, H.Z. Song, J.F. Jia, X. Hu, Prog. Nat. Sci. Mater. Int. 23 (4) (2013) 408–412.
[23] Schlusseltechnologien Key Technologies, 41st IFF Springschool, 2010, A1–A18.